Mechanisms of Calcite Dissolution Using Environmentally Benign Polyaspartic Acid: A Rotating Disk Study

Kathie Burns, You-Ting Wu, and Christine S. Grant*

Department of Chemical Engineering, North Carolina State University, Campus Box 7905, Raleigh, North Carolina 27695-7905

Received September 27, 2002. In Final Form: February 7, 2003

The removal of calcium mineral deposits from metal surfaces is of practical interest for a variety of fields (i.e., food, petroleum, and chemical industries). This study investigated the mechanisms of calcite ($CaCO_3$) dissolution using environmentally benign polyaspartic acid (PASP) under controlled hydrodynamic conditions by a rotating disk technique. The specific role of PASP conformation and surface interactions in the dissolution process was further studied using scanning electron microscopy and dynamic light scattering techniques. Using this combined approach, the dissolution mechanisms were investigated as a function of pH (3.5−10.0), rotating speed (150−1500 rpm), polymer concentration (0.001−0.1 M), and molecular weight (3000 and 10 000 M_w). To quantify the effect of PASP on enhancing calcite dissolution, an enhancement factor, η_{enh}, was defined as a ratio of the rate of dissolution in PASP over the rate in water. Maximum enhancement was observed at pHs in the range 4−5, where an optimal combination of acid attack and chelant attack may appear. Dissolution is governed primarily by interfacial phenomena, including adsorption and surface reactions, at high pHs (>7), while it is controlled by mass transport at low pHs (<7). Increasing polymer concentration under acidic pH conditions, or increasing pH, raises the contribution of the interfacial controlled dissolution mechanism. Dissolution at high pHs is inhibited by small amounts of PASP (0.001−0.01 M) and enhanced by large quantities (0.1 M) of PASP, and proceeds via a surface complexation mechanism involving the chelation of calcium by PASP. A kinetic model incorporating surface adsorption and sequestration chemistry was developed to successfully calculate the dissolution kinetics of calcite at pHs above 7. In contrast, dissolution at low pHs occurs predominantly by acid attack from all acidic species (including H^+ and all partly dissociated PASP species), and PASP enhances dissolution over the entire concentration range (0.001−0.1 M). The lower molecular weight (3000) PASP is the more efficient dissolving agent at low pHs than the higher molecular weight (10 000) PASP. Dissolution at low pHs represents the most complicated case. An analysis of the dissolution mechanisms at low pHs was conducted on the basis of the consideration of mass transfer, polymer surface adsorption, conformation of polymers, and surface interactions.

1. Introduction

1.1. Motivation. The accumulation of calcium mineral deposits on metal surfaces causes significant problems with equipment inefficiency and costs associated with repair and maintenance. Because of the inverse solubility of calcium at elevated temperatures, calcium salts precipitate from aqueous streams during many processes, particularly in the dairy industry, and in other systems such as petroleum oil wells and sedimentation basins.[1,2] These deposits reduce the efficiency of heat exchangers and cooling towers, and often obstruct the fluid flow of oil in pipes during oil recovery procedures. As the global costs for alleviating these fouling problems are enormous, the demand remains for effective cleaning formulations.

Traditionally, strong acids such as hydrochloric and sulfuric acids have been used in calcium scale removal applications. In previous years, inorganic additives were employed as corrosion and scale inhibitors in numerous fields but were gradually replaced by organic materials such as organic phosphates and phosphonates.[3,4] Due to environmental concerns, less toxic materials were investigated for scale inhibition and removal, including poly(acrylic acid) and polyamines.[3] However, poly(acrylic acid) and its derivatives are not biodegradable and are unsuitable for the environment due to their persistence. Deposit removal formulations have also employed chelating agents, which readily dissolve metals by forming water-soluble metal complexes via multiple coordinative bonds. Some common chelants that have been studied for calcium mineral dissolution include EDTA (ethylenediaminetetraacetic acid), acetic acid, and citric acid. However, acetic and citric acids do not form highly stable complexes with calcium, and while EDTA has proven to be an extremely successful calcium chelant, there are environmental concerns about heavy metal mobilization in groundwater sources and non-biodegradability.

In recent years, a nontoxic, environmentally benign polymer, polyaspartic acid (PASP), has been identified as a possible "green" alternative to traditional calcium cleaning agents.[3,5−8] Donlar Corporation was awarded the 1996 Presidential Green Chemistry Challenge Award for developing environmentally safe thermal polyaspartate for use as a scale inhibitor for calcium carbonate, calcium sulfate, and barium sulfate.[3] In a variety of tests, commercial polyaspartates of 3000−30 000 molecular

(1) Fredd, N. C.; Fogler, H. S. *Chem. Eng. Sci.* **1998**, *53* (22), 3863−3874.
(2) Fredd, N. C.; Fogler, H. S. *J. Colloid Interface Sci.* **1998**, *204*, 187−197.
(3) Darling, D.; Rakshpal, R. *Mater. Perform.* **1998**, *37* (12), 42−45.
(4) Tomson, M. B.; Fu, G.; Watson, M. A.; Kan, A. T. Mechanisms of Mineral Scale Inhibition, SPE 74656; *Proceedings of the 4th SPE International Symposium on Oilfield Scale*, Aberdeen, U.K., January 30−31, 2002.
(5) Ashley, S. *Sci. Am.* **2002**, *286* (4), 32−34.
(6) Reisch, M. *Chem. Eng. News* **2002**, *80* (8), 23−23.
(7) Littlejohn, F.; Grant, C. S.; Saez, A. E. *Ind. Eng. Chem. Res.* **2000**, *39* (4), 933−942.
(8) Littlejohn, F.; Grant, C. S.; Saez A. E.; Wong, Y. L. *Ind. Eng. Chem. Res.* **2002**, *41* (18), 4576−4584.

10.1021/la020815g CCC: $25.00
Published on Web 06/06/2003

weight met criteria for ready biodegradability, the most stringent measure of biodegradability.[9] PASP is currently used in various applications, including as a dispersing agent in detergent and paint formulations, and as an antiscalant in oil recovery platforms and agricultural fertilizers.[6,10] In this study, we will look specifically at the role of PASP in the dissolution of calcite and will investigate the mechanisms of this process.

1.2. Mechanisms of Dissolution. Calcite dissolution in various aqueous media has been shown to be limited by one or both of the following mechanisms: (1) reactions occurring at the interface between the liquid and solid deposit, and (2) mass transfer of reacting and/or product species between the bulk solution and the solid mineral surface.[1,11−14] It is reported that, in both the absence and presence of cleaning agents, calcite dissolution in aqueous solutions is generally controlled by mass transport under acidic conditions, by interfacial reactions under basic conditions, and by a combination of the two at intermediate pHs.[1,2,14−17] However, calcite dissolution proceeds via different mechanisms in the presence of water, acidic species, and complexing agents.

Rotating disk studies, which allow mass transfer control under well-defined hydrodynamics,[18−20] have demonstrated that, in the pH range 3−6.2, the dissolution of calcite in water is controlled by both the flux of hydrogen to the calcite surface and the reaction of water with calcite at the solid−liquid interface.[15] In solutions of KCl, dissolution was found to be diffusion-limited below pH ∼ 4−5.5 and influenced by interfacial kinetics above this pH.[14,21] Rotating disk experiments have also determined that calcite dissolution in HCl, a strong acid, is governed by the rate of H^+ transport.[11] In the presence of acetic acid, a weak acid, the calcite dissolution rate is dependent on the transport of reactants to the interface, the kinetics of the surface reaction, and the transport of products away from the interface.[1] The thermodynamics of the reversible surface reaction were found to significantly influence the overall rate of dissolution due to the surface dissociation of the weak acid. Additional rotating disk studies have shown that dissolution of calcite using chelating agents such as EDTA and citrate is diffusion-controlled at low pH and reaction-limited at high pH.[1,2] The rate of dissolution in chelating agents depends on the stability of the metal−chelate complexes formed during dissolution.

The goal of the present research is to evaluate the role of environmentally benign PASP in enhancing the dissolution of calcite and to determine the influence of mass transport on dissolution. PASP is an effective calcium chelant and has been shown both to inhibit crystallization of calcium salts and to promote dissolution of calcium minerals under various conditions.[22−25] A study done by our group investigated the effect of PASP on the dissolution of the calcium phosphate minerals DCPD (brushite) and HAP (hydroxyapatite)/DCPD under turbulent flow conditions. Dissolution was enhanced at alkaline pHs over a wide range of PASP concentrations and at low pHs from moderate to high PASP concentrations.[8] It was concluded that PASP accelerates the rate of calcium phosphate removal via calcium sequestration during the interfacial dissolution step.

In a separate study by our group, batch dissolution experiments involving calcium carbonate powder further demonstrated the ability of PASP as an effective sequestrant for $CaCO_3$.[23] PASP was found to increase the rate of $CaCO_3$ dissolution as compared to the rate in water over a range of pH and PASP concentrations. However, as hydrodynamics in a batch system are not well-characterized, it is difficult to resolve the mechanism of dissolution for this case. Combining results from previous batch experiments and current rotating disk studies will enable a complete analysis of the contributions of surface reaction and mass transfer to the overall rate of calcite dissolution. This approach will also allow the calculation of an enhancement factor to quantify the effect of PASP on dissolution rate. However, it is first necessary to understand the fundamentals of transport, PASP chelation chemistry, and polymer configuration in order to develop a comprehensive picture of the dissolution process.

2. Theory

2.1. Mass Transport. The following expression describes the diffusive flux (J_{MT}) of a reacting species to the surface of a rotating disk under laminar flow ($Re < \sim 3 \times 10^5$) through the solution of the Navier−Stokes and continuity equations:[2,26−28]

$$J_{MT} = \frac{0.6205 Sc^{-2/3} (\omega \nu)^{1/2}}{1 + 0.2980 Sc^{-1/3} + 0.1451 Sc^{-2/3}} (C_b - C_i) = k_m (C_b - C_i) \quad (1a)$$

where the Schmidt number, $Sc = \nu/\mathscr{D}$, ν and $\mathscr{D}$ are the kinematic viscosity and effective diffusion coefficient of the reacting species (e.g. H^+ or H_mL), and ω is the rotating speed of the disk. This solution is valid for high Schmidt numbers, large reaction vessel volume, and negligible disk edge effects. These criteria are maintained in the current work. In this expression, the flux is proportional to a concentration gradient ($C_b - C_i$) and an overall mass transfer coefficient, k_m. It is important to note the dependence of the flux on the square root of ω, the rotating speed. For systems where the rate of mass transport is the rate-limiting step, the overall rate of dissolution is equal to the mass flux and is therefore linearly dependent

(9) Ross, R. J.; Low, K. C.; Shannon, J. E. *Mater. Perform.* **1997**, *36* (4), 53−57.
(10) Wang, X.; Lee, B. I.; Mann, L. *Colloids Surf., A: Physiochem. Eng. Aspects* **2002**, *202* (1), 71−80.
(11) Lund, K.; Fogler, H. S.; Mccune, C. C.; Ault, J. W. *Chem. Eng. Sci.* **1975**, *30*, 825−835.
(12) Liu, Z.; Dreybrodt, W. *Geochim. Cosmochim. Acta* **1997**, *61* (14), 2879−2889.
(13) Liang, Y.; Baer, D. R. *Surf. Sci.* **1997**, *373*, 275−287.
(14) Sjöberg, E. L.; Rickard, D. T. *Chem. Geol.* **1984**, *42*, 119−136.
(15) Compton, R. G.; Daly, P. J. *J. Colloid Interface Sci.* **1984**, *101* (1), 159−166.
(16) Plummer, L. N.; Wigley, T. M.; Parkhurst, D. L. *Am. J. Sci.* **1978**, *278*, 179−216.
(17) Compton, R. G.; Pritchard, K. L.; Unwin, P. R. *Freshwater Biol.* **1989**, *22*, 285−288.
(18) Kabin, J. A.; Withers, S. T.; Grant, C. S.; Carbonell, R. G.; Saez, A. E. *J. Colloid Interface Sci.* **2000**, *228* (2), 344−358.
(19) Kabin, J. A.; Saez, A. E.; Grant, C. S.; Carbonell, R. G. *Ind. Eng. Chem. Res.* **1999**, *38* (3), 683−691.
(20) Beaudoin, S. P.; Grant, C. S.; Carbonell, R. G. *Ind. Eng. Chem. Res.* **1995**, *34* (10), 3307−3317.
(21) Compton, R. G.; Daly, P. J. *J. Colloid Interface Sci.* **1987**, *115* (2), 493−498.
(22) Sikes, C. S.; Yeung, M. L.; Wheeler, A. P. In *Surface Reactive Peptides and Polymer: discovery and commercialization*; Sikes, C. S., Wheeler, A. P., Eds.; American Chemical Society: Washington, DC, 1991; p 50.
(23) Wu, Y.-T.; Grant, C. S. *Langmuir.* **2002**, *18* (18), 6813−6820.
(24) Littlejohn, F.; Saez, A. E.; Grant, C. S. *Ind. Eng. Chem. Res.* **1998**, *37*, 2691−2700.
(25) Littlejohn, F. Ph.D. Dissertation, North Carolina State University, Raleigh, NC, 1999.
(26) Lund, K.; Fogler, H. S.; Mccune, C. C. *Chem. Eng. Sci.* **1973**, *28*, 691−700.
(27) Levich, V. G. *Physiochemical Hydrodynamics*; Prentice-Hall: Englewood Cliffs, NJ, 1962.
(28) Newman, J. *J. Phys. Chem.* **1966**, *70* (4), 1327−1328.

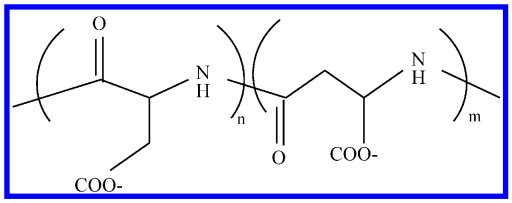

Figure 1. Structure of polyaspartate $(C_4H_4NO_3)_x$.

on $\omega^{1/2}$. For systems where dissolution is dominated by reaction kinetics, the dissolution rate is independent of ω.

However, for a system where both mass transfer and reactions contribute to the dissolution, the overall rate of dissolution should be expressed by Koutecky−Levich analysis:[29]

$$\frac{1}{J_T} = \frac{1}{k_{app}C_r} + \frac{1}{k_m^* C_r \omega^{1/2}} \qquad (1b)$$

where $k_m^* = k_m/\omega^{1/2}$ is independent of ω (see eq 1a), C_r is the bulk concentration of the reactant, and k_{app} is the apparent heterogeneous rate constant. In eq 1b, the reciprocal dissolution rate, $1/J_T$, is expressed as a linear function of $\omega^{-1/2}$, which was known as a Koutecky−Levich plot. k_{app} can be calculated from the intercept of a Koutecky−Levich plot, and k_m^*, from the slope. The total resistance $(1/\kappa)$ for the dissolution process is the sum of $1/k_{app}$ and $1/k_m$. The current research will use both theories to analyze the experimental data of calcite dissolution.

2.2. Chelation Chemistry. Polyaspartic acid serves as a calcium chelating agent by forming stable, water-soluble complexes through coordination bonds with calcium ions. Functional groups located along the polymer chain surround calcium ions and extract them from the salt crystal lattice in a secure metal−ligand complex. The chelating ability of PASP arises from the presence of the carboxyl groups in each polymer segment, as illustrated in the structure of PASP (Figure 1).

Figure 1 represents two repeating segments, *n* and *m*, of polyaspartate, which are randomly distributed along the backbone of the polymer. The total number of units will depend on the molecular weight. For instance, there are approximately 72 segments in a 10 000 (weight average) molecular weight sodium polyaspartate (Na-PASP) chain and 22 segments in a 3000 MW Na-PASP chain for an equivalent molecular weight of 137 for each segment. Thus, the overall chelating ability of the species will be a function of molecular weight. It has been reported that the most effective range of PASP molecular weight for calcium scale inhibition is 1000−4000 MW.[9] Therefore, this study will compare the dissolution efficiencies for 3000 and 10 000 MW PASP products.

A hypothetical "effective chelating unit" of PASP is modeled as four residues, consisting of four carboxyl groups. This is related to the titration chemistry of PASP, where deprotonation occurs gradually through many consecutive dissociation steps. Silverman et al.[30] discovered that it is possible to accurately model the deprotonation of PASP as a series of four subsequent dissociation steps, by assuming four p*K* values. Thus, using this model of four p*K* values, the species distribution plot in Figure 2 was constructed from data of titration experiments done in our group.[23]

(29) Koutecky, J.; Levich, V. G. *Zh. Fiz. Khim.* **1958**, *32*, 1565.
(30) Silverman, D. C.; Kalota, D. J.; Stover, F. S. *Corrosion* **1995**, *51* (11), 818−825.

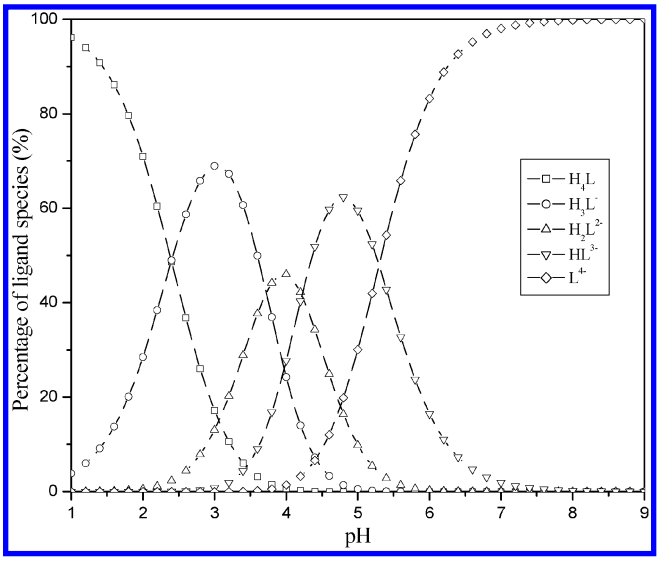

Figure 2. Theoretical PASP species distribution plot.[23]

Table 1. Polyaspartic Acid Dissociation and Calcium Complexation Reactions

	− log K_{eq} (25 °C)
PASP Dissociation: ($K_{A,m}$)	
$H_4L \leftrightarrow H^+ + H_3L^{1-}$	2.27,[a] 2.2[c]
$H_3L^{1-} \leftrightarrow H^+ + H_2L^{2-}$	3.60,[a] 3.6[c]
$H_2L^{2-} \leftrightarrow H^+ + HL^{3-}$	4.09,[a] 4.3[c]
$HL^{3-} \leftrightarrow H^+ + L^{4-}$	5.17,[a] 5.4[c]
Calcium−Polymer Complexation: ($K_{B,m}$)	
$Ca^{2+} + L^{4-} \leftrightarrow CaL^{2-}$	3.02,[a] 2.88[b]
$Ca^{2+} + HL^{3-} \leftrightarrow CaHL^{1-}$	2.55,[a] 2.47[b]
$Ca^{2+} + H_2L^{2-} \leftrightarrow CaH_2L$	2.16,[a] 2.14[b]

[a] Values for 10 000 MW PASP determined by Wu and Grant.[23] [b] Values for 3000 MW PASP determined by titration experiments in this work. [c] Values for 9200 MW PASP determined by Silverman et al.[30]

Figure 2 illustrates that, at a specific pH, there are multiple polymer species present in solution. The behavior of these individual species and their cooperative influence on the rate of dissolution are crucial to understanding the dissolution process. Table 1 summarizes the PASP dissociation and complexation reactions that occur during calcite dissolution.

In Table 1, $K_{A,m}$ are the theoretical p*K* values of PASP and $K_{B,m}$ represent binding constants for calcium−polymer complexation. These values are important for calculating interfacial reaction rates during calcite dissolution at various pH's. Combining this information with mass transport rates calculated from rotating disk results will enable a theoretical prediction of overall calcite dissolution in PASP. To investigate the effect of pH on interfacial dissolution, we evaluate the dominant PASP species and significant reactions that occur for three representative pH conditions.

In general, one or a combination of the following reactions dominates calcite dissolution in aqueous PASP solution, depending on pH.

Proton attack:

$$H^+ + CaCO_3 \leftrightarrow Ca^{2+} + HCO_3^{1-} \qquad (2)$$

Water attack:

$$H_2O + CaCO_3 \leftrightarrow Ca^{2+} + CO_3^{2-} + H_2O \qquad (3)$$

Ligand attack:

$$L^{4-} + CaCO_3 \leftrightarrow CaL^{2-} + CO_3^{2-} \quad (4a)$$

$$HL^{3-} + CaCO_3 \leftrightarrow CaL^{2-} + HCO_3^{1-} \quad (4b)$$

$$H_2L^{2-} + CaCO_3 \leftrightarrow CaHL^{1-} + HCO_3^{1-} \quad (4c)$$

$$H_3L^{1-} + CaCO_3 \leftrightarrow CaH_2L^{2-} + HCO_3^{1-} \quad (4d)$$

Reaction 2 is significant at low pH (below ≈ pH 4−5), while the water (eq 3) and ligand (eq 4) reactions dominate at higher pH values.[2,14−17] The contribution of each ligand reaction (eqs 4a−d) depends on the polymer species distribution (Figure 2), which is also closely related to pH.

2.2.1. pH 10. Above pH ∼ 6, according to the species distribution plot, the primary free PASP species in solution is L^{4-}. Thus, at pH 10, reactions 3 and 4a dominate the interfacial dissolution process. The individual contributions of the two reactions to the overall dissolution rate will depend on the concentration of PASP ligand, with the water reaction dominating at low PASP concentration and the ligand reaction dominating at high PASP concentration.

Since calcite dissolution in aqueous media is generally controlled by interfacial reaction kinetics at high pH, reactions 3 and 4a are considered the rate-determining steps. With this in mind, a model has been developed to predict the dissolution of calcite in PASP at pH 10, which is a pH of interest, since alkaline detergents are generally optimal for soil removal in cleaning applications.[31] The overall rate of reaction (r_T) is the sum of the rates of the water (r_w) and ligand (r_L) reactions:

$$r_T = r_w + r_L \quad (5)$$

where r_w and r_L are given by

$$r_w = k_w\theta_c\theta_a(1 - [Ca^{2+}]_{(i)}[CO_3^{2-}]_{(i)}/K_{sp}) \quad (6)$$

$$r_L = k_L K_L \theta_c \theta_a([L^{4-}]_{(i)} - [CaL^{2-}]_{(i)}[CO_3^{2-}]_{(i)}/K_{eq}) \quad (7)$$

In eqs 6 and 7, k_w and k_L are the surface reaction rate constants for water and ligand with calcite, and K_L is the adsorption equilibrium constant for PASP ligand. θ_c and θ_a are the fractions of cationic and anionic adsorption sites, respectively. K_{sp} is the solubility product for calcium carbonate, and K_{eq} is the product of K_{sp} and the Ca−L binding constant, $K_{B,1}$. Equations 6 and 7 are derived from Langmuir−Hinshelwood adsorption kinetics, following the work of Fredd and Fogler,[2] and Wu and Grant.[23]

At steady state, the net rate of reaction is equal to the rate of calcium transport from the interface to the bulk. This is expressed as

$$r_T = k_m([Ca]_{T,i} - [Ca]_{T,b}) \quad (8)$$

where $[Ca]_{T,i}$ and $[Ca]_{T,b}$ are the interfacial and bulk concentrations of total calcium, respectively. Solving eqs 5−8 simultaneously using equilibrium values from Table 1 and the literature,[1] model parameters for reaction rate constants and ligand adsorption equilibria may be calculated to yield a theoretical dissolution rate. A comparison of the model to experimental rate data is included in the results section.

(31) http://www.novozymes.com/eventure/demo/b077d-gb.pdf (September 3, 2002).

2.2.2. pH 5. At pH 5, the principal polymer species in solution (see Figure 2) are HL^{3-} (60% of total PASP) and L^{4-} (30%), with H_2L^{2-} constituting the remainder (10%). Thus, in the presence of these species, reactions 4b and 4c begin to influence the dissolution rate, in addition to reactions 3 and 4a. Furthermore, at this lower pH, the reaction between hydrogen and calcite (eq 2) becomes important, and dissolution is partly limited by the mass transport of H^+. Consequently, it is trivial to predict dissolution behavior at pH 5 with a kinetic model. In this case, the Koutecky−Levich analysis[29] can be applied to estimate how mass transfer and interfacial reactions contribute to the dissolution.

2.2.3. pH 3.5. The dominant forms of PASP ligand at pH 3.5 are H_3L^{1-} (56% of total ligand species) and H_2L^{2-} (33%). In this regime, dissolution is again complicated by the presence of several polymer species which each react with calcium. Dissolution is strongly dependent on the rate of H^+ transport as well as the mass transport of chelating species to the interface. As with pH 5, the Koutecky−Levich analysis[29] can be used to determine the contributions of mass transfer and interfacial reactions to the dissolution process.

2.3. Polymer Conformation and Adsorption. The rate of mineral dissolution in the presence of PASP is also dependent on the conformation of polymer molecules in solution and at the solid−liquid interface. Solution pH has a strong influence on the solvent conditions, which determine whether the polymer chains are extended or coiled. Consequently, pH affects the size and configuration of polymer molecules as well as the transport properties of the polymer.

Polymer chain length also affects the transport properties of the molecules. As a general rule, the translational diffusion coefficient, D, of the polymer is related to molecular weight, MW, as[32]

$$\mathscr{D} \propto MW^{-\alpha} \quad (9)$$

where α is a measure of solvent quality and ranges from about 0.5−0.6, for theta to good solvent conditions.[32] Thus, polymer chains of lower molecular weight should diffuse through a solvent faster than those of higher molecular weight.

The extent of polymer adsorption onto a solid surface (e.g. calcite) is also heavily influenced by pH, which governs the swollen or contracted nature of the polymer chains at the interface. Some segments of the polymer may attach to the substrate in a flat configuration, and other segments may protrude from the surface. Studies have shown that adsorption of polyelectrolytes such as PASP onto calcium minerals is generally favorable at low pH,[10,33−35] and the polyelectrolytes likely adopt a flat conformation on the mineral surfaces. One study demonstrated that PASP adsorbs onto hydroxyapatite (a form of calcium phosphate) in a relatively flat configuration, with train and loop segments.[33] Results from a separate study suggested that PASP adsorbs strongly onto calcite in a flat conformation.[36]

Using dynamic light scattering (DLS) techniques, the translational diffusion coefficient, $\mathscr{D}$, of a polymer in

(32) Doi, M. *Introduction to Polymer Physics*; Oxford University Press: 1996.

(33) Tsortos, A.; Nancollas, G. H. *J. Colloid Interface Sci.* **1999**, *209*, 109−115.

(34) Chang, H.-C.; Healy, T. W.; Matijevic, E. *J. Colloid Interfacial Sci.* **1983**, *92* (2), 469−478.

(35) Schaad, P.; Thomann, J. M.; Voegel, J. C.; Gramain, P. *Colloids Surf., A: Physiochem. Eng. Aspects* **1994**, *83*, 285−292.

(36) Wierzbicki, A.; Sikes, C. S.; Madura J. D.; Drake, B. *Calcif. Tissue Int.* **1994**, *54*, 133−141.

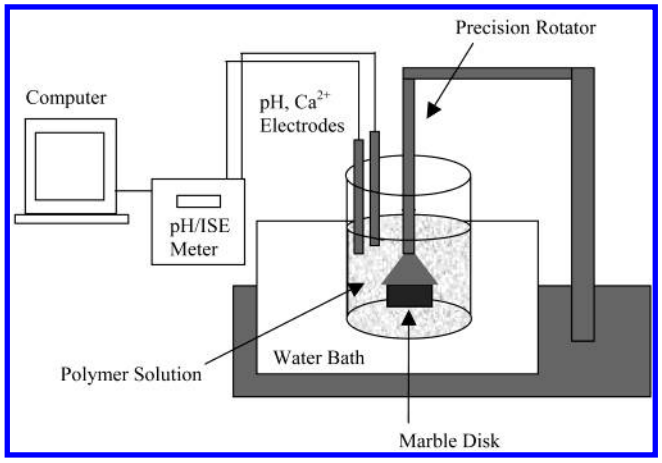

Figure 3. Rotating disk experimental apparatus.

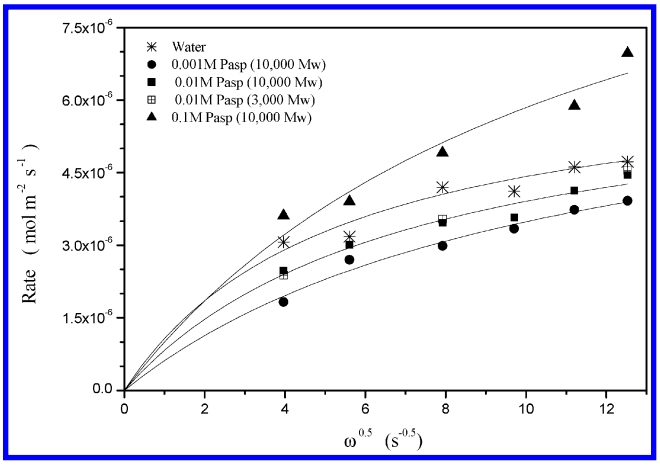

Figure 4. Rate of calcite dissolution versus square root of rotational speed with and without PASP at pH = 10.

solution can be directly measured under various conditions of pH, polymer concentration, and molecular weight. From these experiments, values for $\mathcal{D}$ can be used to estimate the hydrodynamic radius, R_H, the effective size of polymer chains in solution. R_H indicates how coiled the polymer molecules are in solution including solvent effects. Thus, DLS studies are useful for a qualitative understanding of the dynamic behavior of PASP in solution and at the interface during dissolution.

3. Experimental Methods

3.1. Materials. Sodium polyaspartate samples (40 wt % solids, >95% purity, pH = 8−9.5) of weight average molecular weights (MW) 10 000 and 3000 were provided by Donlar Corporation. Calcium standard solution (0.1 M) was obtained from Fisher Scientific for calcium ion electrode calibration. Calcite marble of 96% purity (determined analytically in this study) was supplied by the Durham Marble Company. All other reagents and solutions were analytical grade, and water was deionized.

3.2. Equipment. Rotating disk studies were performed using a Pine Instruments Rotating Disk apparatus (Figure 3), equipped with Pine Instrument MSRX Speed Control. The temperature of the water bath surrounding the polymer solution was controlled using a Fisher Scientific Isotemp model 730 immersion circulator thermostat. Calcium ion (Ca^{2+}) and pH data were measured with a Denver Instrument model 225 pH/ISE meter (Orion pH probe and calcium ion selective electrode model 97−20 ion*plus*). Continuous (Ca^{2+}) and pH readings were recorded on a computer using Winwedge software. Total calcium concentrations were determined using a Perkin-Elmer AAnalyst 100 atomic absorption spectrometer, operated with AAWinLab software. Scanning electron images were obtained using a Hitachi 3400 environmental scanning electron microscope, operated at beam voltages of 4−15 kV. Dynamic light scattering experiments were performed using a 200 megawatt argon laser light source, a Brookhaven Instruments PMT 9836 photomultiplier detector positioned at a scattering angle of 90°, and a Brookhaven Instruments 9000 AT autocorrelator and software (9kdlsw version 2.15) for data acquisition.

3.3. Method. Calcite disks were prepared on the basis of techniques described in earlier research.[1,2,12,15] In summary, disks were cut to 3.2 cm diameter and 1.5 cm thickness from a marble core and polished to 3000 mesh surface smoothness using 150, 300, 600, 1000, and 3000 mesh (8 μm) polishing disks successively. To isolate the top surface of the disks for solution exposure, the sides of the disks were coated with a polystyrene−CCl_4 solution. The disks were attached to the rotor shaft by gluing a magnetic insertion piece to the bottom of the disks using an epoxy resin. All disks were rinsed with DI water prior to experimentation.

Polyaspartic acid solutions (0.001, 0.01, and 0.1 M) were prepared by diluting sodium polyaspartate (40 wt % stock solution) to 800 mL of total volume using DI water. KCl was added to maintain a constant solution ionic strength (I) of 0.2 M. Solutions without polymer also contained KCl for constant I. Upon stirring and allowing the mixture to reach ambient temperature, solution pH was adjusted manually via dropwise addition of HCl or NaOH.

A beaker containing the polymer solution was placed in a water bath maintained at 25 ± 0.5 °C, and the calcite disk was then immersed into the solution to a height of approximately 4 cm from the bottom of the reaction vessel to avoid edge effects. The pH and Ca^{2+} ISE electrodes were then placed in the solution for bulk measurements. The disk was rotated at the desired speed between 150 and 1500 rpm (equivalent to $3.8 \times 10^4 < Re < 3.8 \times 10^5$) for 30−60 min. Bulk fluid samples were obtained every 2 min using a 2 mL syringe and were subsequently analyzed for total calcium concentration using the atomic absorption spectrometer.

Profiles for total calcium concentration and free calcium concentration were plotted as a function of time. Dissolution rates were calculated directly from the initial linear slopes of the total calcium concentration plots.

4. Results and Discussion

4.1. Governing Mechanisms of Calcite Dissolution at Different pHs. Dissolution results are divided into three pH regimes (pH 10, 5, and 3.5) corresponding to a study of the different dominating polymer ligand species in solution. According to eqs 1a and 1b, plotting dissolution rate (r_T) versus $\omega^{0.5}$ or $1/r_T$ versus $\omega^{-0.5}$ yields information about the governing mechanisms for calcite dissolution. These graphs are shown in Figures 4 and 7−9 for dissolution at pH 10, 5, and 3.5, respectively, over the range of rotating speeds (150−1500 rpm) and spanning 3 orders of magnitude of polymer concentration (0.001−0.1 M). Results are also shown for water containing 0.2 M KCl. Experiments are highly reproducible, since disks were finely polished and initial rates were used to avoid discrepancies due to possible changes in surface morphology.

4.1.1. pH 10. Dissolution rates at pH 10 (Figure 4) are presented for water, three concentrations of 10 000 MW PASP, and an intermediate concentration of 3000 MW PASP at low, intermediate, and high ω values. A nonlinear relationship between rate and $\omega^{0.5}$ is observed for each concentration of PASP, indicating that dissolution is governed primarily by the reactions at the solid−liquid interface. These reactions involve a series of adsorption and surface complexation reactions between calcium and PASP ligand, as described by eqs 4a−d.

At high pH, dissolution is inhibited by the presence of small amounts of PASP, as rates are lower in 0.001 and 0.01 M PASP than in water. However, as PASP concentration increases, the rate exceeds the rate in water, and dissolution is enhanced at 0.1 M PASP. This agrees with

similar studies of calcite dissolution in dicarboxylic acid solutions, where dissolution was inhibited at concentrations below ~0.01 M.[37] Inhibition was attributed to the blocking of dissolution sites by the adsorbed dicarboxylic acid species. In the presence of acetic acid, which is a weak acidic species such as PASP, calcite dissolution was found to be limited by the transport of product species away from the surface.[1]

For the case of PASP, dissolution at high pH is limited by each step of the interfacial dissolution process, including adsorption, complexation, and desorption. Since calcium minerals typically adopt a negative surface charge due to OH^- adsorption at pHs > 9.0−9.5,[38] adsorption of anionic PASP molecules is relatively slow, resulting in a low interfacial ligand concentration, $[L]_i$. Consequently, the ligand reaction with calcite (eq 7) is inhibited, generating a small amount of Ca-PASP product, $[Ca]_{T,i}$. The low interfacial concentration of calcium product is not sufficient to drive the transport of species to the bulk (eq 8). Thus, dissolution is inhibited until a high enough surface concentration of PASP is attained.

Interfacial limitations to dissolution are further supported by dynamic light scattering (DLS) results obtained in this study. From DLS experiments, the diffusion coefficients of 0.001 M aqueous solutions of 3000 and 10 000 MW PASP were measured as 6.4×10^{-6} and 5.0×10^{-6} cm^2/s, respectively, corresponding to hydrodynamic radii of 0.34 and 0.53 nm. While the values for D seem rather high and those for R_H seem rather low for polymer molecules in aqueous solution, they are reasonable due to the presence of added salt in solution, which screens Coulombic interactions between charged polymeric species.[31,39] The ionic strength of 0.2 M used in the dissolution and DLS experiments could account for the collapse of polymer chains, leading to large diffusion coefficients. These high D values also suggest that molecules are transported rapidly to the calcite interface, such that mass transfer is not a rate-limiting step. Also, the extremely low values of R_H imply that the PASP chains are tightly coiled in solution, which may lead to loop and tail configurations at the interface. These conformations are not favorable for strong adsorption. On the other hand, it is also possible that R_H is much smaller than the radius of gyration, R_g, which is a measure of the polymer size based on the center of mass. If this is the case, a large R_g would suggest that water flows freely through the polymer coils, meaning that water is a good solvent for PASP and the chains are actually extended. In a good solvent, it is favorable for the molecules to remain in solution, so that adsorption requires a large amount of energy. In either case, the DLS results indicate that dissolution at pH 10 is controlled by interfacial interactions, including the adsorption process.

In addition, dissolution rates are comparable for 3000 and 10 000 MW at pH 10. This is because dissolution is not largely dependent on diffusion but rather depends on the surface reaction kinetics. Comparing values for the calcium binding constants of 3000 and 10 000 MW PASP from Table 1, it is apparent that the extent of complexation is similar for the two molecular weights. Therefore, under surface reaction control, the polymer molecular weight has a negligible effect on the overall rate of dissolution.

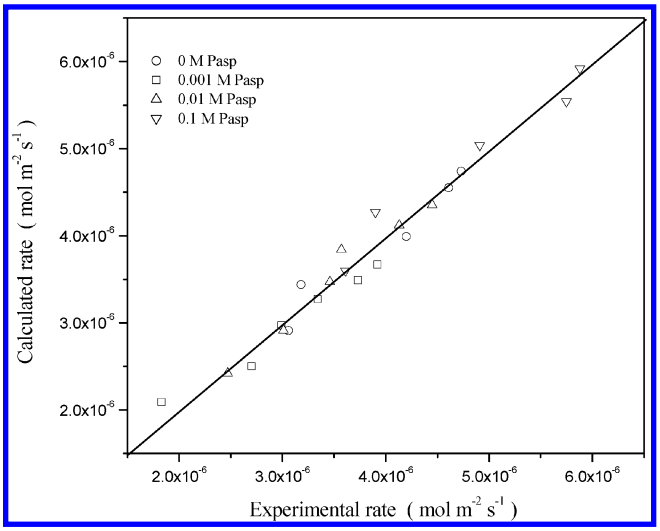

Figure 5. Theoretical versus experimental dissolution rate at pH = 10.

Table 2. Model Parameters for Calcite Dissolution in PASP Solutions (pH = 10)

k_w[a]	k_L[a]	K_L[b]	K_{CaL}[b]
9.6×10^{-6}	9.33×10^{-5}	2.8×10^{2}	2.9×10^{5}

[a] mol m^{-2} s^{-1}. [b] dm^3 mol^{-1}.

Comparisons of theoretical and experimental rates at pH 10 are shown in Figure 5. The solid diagonal line represents a perfect correlation between calculated and experimental dissolution rates. Theoretical data were calculated from the model previously described, and they agree closely with experimental data. The model adequately predicts dissolution rates at high pH over the ranges of ω, PASP concentration, and molecular weights studied, using the model parameters, k_w, k_L, K_L, and K_{CaL}, in Table 2. The parameter K_{CaL} appears in the calculation of θ_c in eqs 6 and 7.[23] Adsorption equilibrium constants for other species included in θ_c and θ_a were estimated from the literature[40] (1000, 3×10^4, and 700 dm^3 mol^{-1} for K_{Ca}, K_{CO_3}, and K_{OH}, respectively). Calculation shows that interfacial reactions contribute 91% (0.001 M PASP) to 99% (0.1 M PASP) of the total resistance to the dissolution process, which agrees well with the experiments.

Using the same model, contributions of the competing water and ligand reactions with calcite at pH 10 were determined and are presented in Figure 6. As shown in the graph, at high PASP concentration, the ligand reaction dominates dissolution, whereas, at low PASP concentration, the water reaction with the surface is dominant.

4.1.2. pH 5. Rotating disk results for pH 5 (Figure 7) are shown for both molecular weights at all concentrations except the lowest (0.001 M), where the two molecular weights exhibit nearly identical dissolution curves. Dissolution is enhanced in the presence of PASP for both 0.01 and 0.1 M concentrations and is comparable to the rate in water for 0.001 M PASP.

The linear dependence of the rate on $\omega^{0.5}$ at the concentrations 0, 0.001, and 0.01 M PASP demonstrates mass transfer control under these conditions. This implies that dissolution is governed by the rate of H^+ and PASP diffusion to the solid−liquid interface, which agrees with literature reports that calcite dissolution is generally diffusion-limited at low pH. At high PASP concentration

(37) Compton, R. G.; Brown, C. A. *J. Colloid Interface Sci.* **1995**, *170*, 586−590.
(38) Holmgren, A.; Wu, L. M.; Forsling, W. *Spectrochim. Acta, A: Mol. Biomol. Spectrosc.* **1994**, *50* (11), 1857−1869.
(39) Grosberg, A. IU.; Khokhlov, A. R. *Statistical Physics of Macromolecules*; AIP Press: New York, 1994.
(40) Compton, R. G.; Brown, C. A. *J. Colloid Interface Sci.* **1994**, *165*, 445−449.

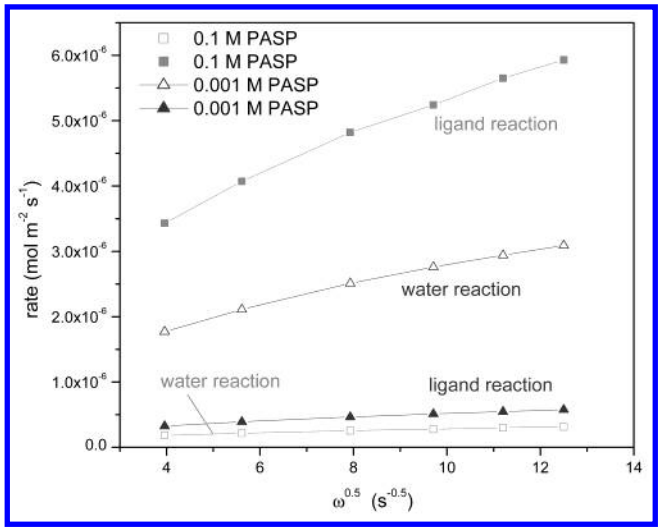

Figure 6. Theoretical contributions of PASP ligand (r_L) and water (r_w) reactions to dissolution at pH 10 calculated from eqs 5 and 6.

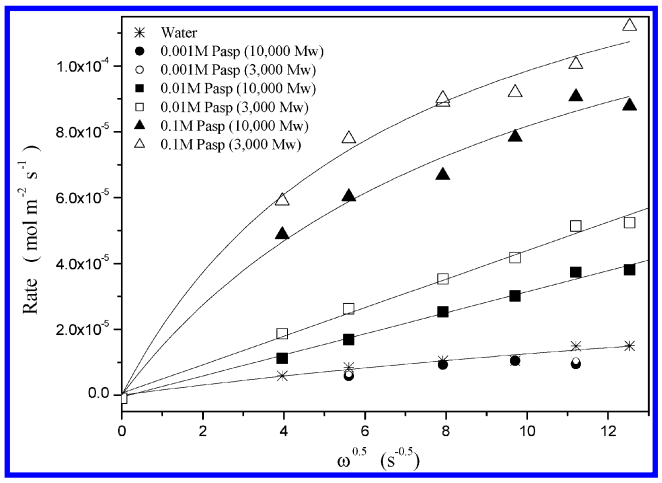

Figure 7. Rate of calcite dissolution versus square root of rotational speed with and without PASP at pH = 5.

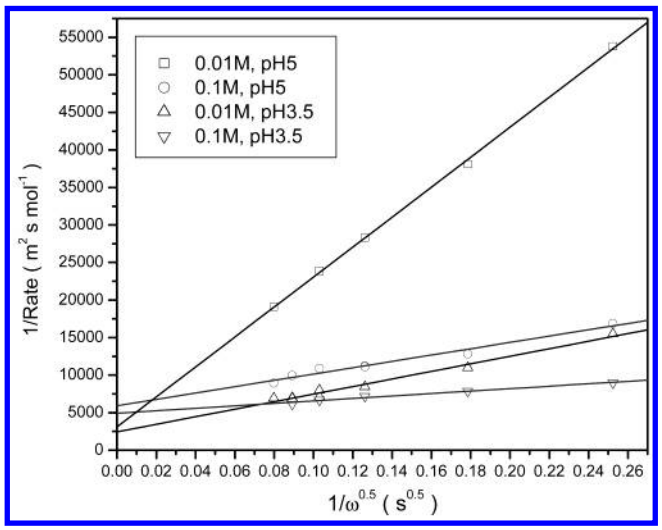

Figure 8. Koutecky−Levich plots of reciprocal rate of calcite dissolution in PASP (3000 MW) versus $1/\omega^{0.5}$ at two concentrations (0.01 M, 0.1 M) and two pHs (3.5, 5).

(0.1 M), the nonlinear correlation between rate and $\omega^{0.5}$ suggests additional limitations due to interfacial reaction. Using the Koutecky−Levich analysis (Figure 8), it is found that interfacial reactions contribute 15% (0.01 M PASP)

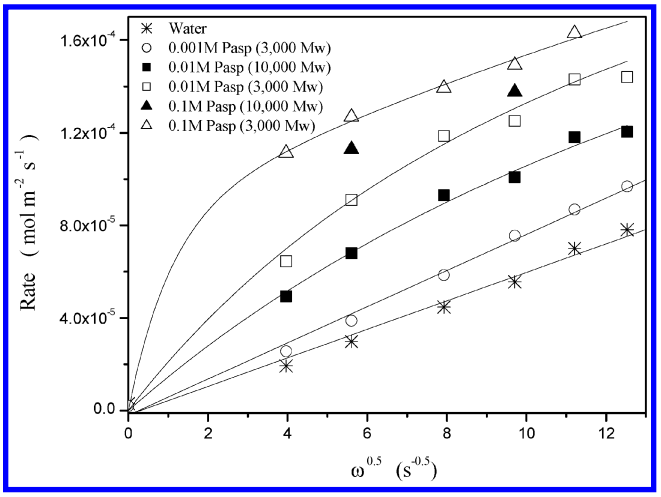

Figure 9. Rate of calcite dissolution versus square root of rotational speed with and without PASP at pH = 3.5.

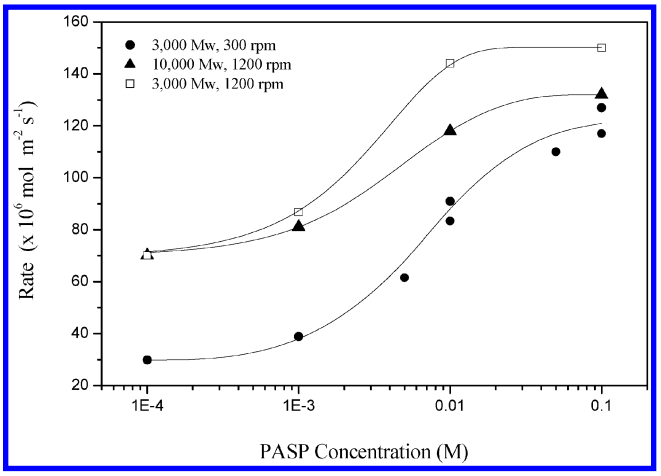

Figure 10. Rate versus PASP concentration at pH 3.5.

to 63% (0.1 M PASP) of the total resistance (calculated from the intercepts and slopes of the Koutecky−Levich plots in Figure 8) to the dissolution.

This transition to a more surface-reaction-limited regime is likely related to adsorption. At low pH (<6), calcium minerals adopt a positive surface charge.[38] Thus, it is likely that adsorption of PASP onto calcite is rapid due to electrostatic interactions between the carboxyl groups of PASP and the positively charged calcite surface. At low and moderate concentrations of PASP, the polymer molecules adopt a flat configuration on the calcite surface. However, as the ligand concentration increases, polymer segments begin to adsorb along the surface in more loop and tail arrangements, slowing the rate of adsorption, forming a thicker diffuse layer, and thus causing a lower efficiency of interfacial reactions than that of mass transport.

Dissolution proceeds more rapidly in solutions of 3000 molecular weight PASP than 10 000 MW. Since dissolution is limited primarily by mass transport at this pH, dissolution is enhanced as the diffusion coefficient of the reactant increases (larger $\mathscr{D}$ increases k_m). Referring back to eq 9, the diffusion coefficient of a polymer species is inversely proportional to the molecular weight ($\mathscr{D} \sim MW^{-\alpha}$). Thus, smaller molecules (i.e. lower MW or tightly coiled chains) travel faster to the calcite interface than larger molecules, thereby increasing the rate of dissolution. In addition, interfacial dissolution is faster for lower MW species, because adsorption is energetically favored for smaller chains. Using atomic force microscopy, Sikes and

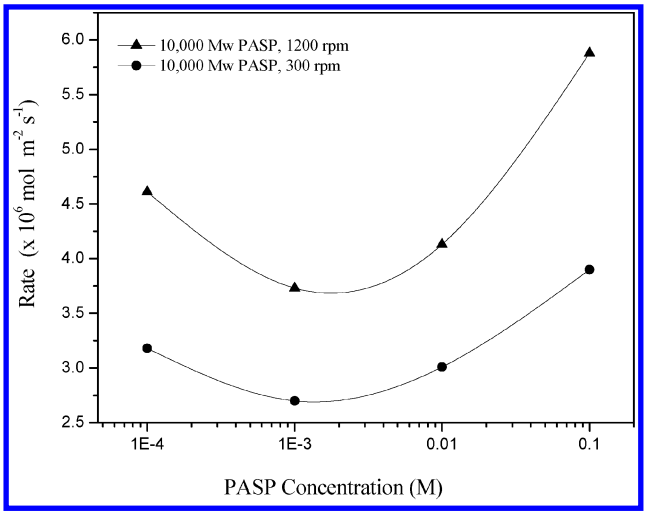

Figure 11. Rate versus PASP concentration at pH 10.

Wierzbicki[41] determined that the energy required for PASP molecules to bind to calcite was approximately twice as large for chains with 45 residues than for those with only 15 monomer units. Therefore, adsorption of 3000 MW PASP is stronger than adsorption of the 10 000 MW species.

4.1.3. pH 3.5. Dissolution rates at pH 3.5 (Figure 9) are shown for water, three concentrations of 3000 MW PASP, and the intermediate concentration (0.01 M) of 10 000 MW PASP. Since trends for the two molecular weights at 0.01 M are similar, data for 0.001 M and 0.1 M 10 000 MW PASP are also expected to follow curves similar to those for 3000 MW PASP, as they do at pH 5 (Figure 7). This is verified by the data at 300 and 900 rpm for 0.1 M 10 000 MW PASP, which lie directly below the same data for 3000 MW PASP, indicating comparable dissolution behavior at the high concentration.

At this pH, dissolution proceeds on a much faster time scale than at pH 5 and 10, and dissolution rates are 1−2 orders of magnitude higher than those for pH 10. PASP increases the rate of calcite dissolution compared to the rate in water for all concentrations, even at 0.001 M. At zero and 0.001 M PASP, dissolution is mass-transfer-limited. At the middle concentration (0.01 M), the slight curvature of the rate versus $\omega^{0.5}$ plot indicates that while mass transport is still a limiting mechanism, interfacial phenomena also begin to influence dissolution. As PASP concentration increases to 0.1 M, the nonlinear nature of the data illustrates the increasing role of surface interaction. Similarly, the Koutecky−Levich analysis in Figure 8 indicates that 35% (0.01 M PASP) to 78% (0.1 M PASP) of total resistance (calculated from the intercepts and slopes of the Koutecky−Levich plots) is contributed from the interfacial reactions.

Finally, 3000 MW PASP results in higher rates of dissolution than 10 000 MW, owing to the faster diffusion of lower molecular weight species. This is consistent with our DLS results, where the diffusion coefficients for 3000 MW and 10 000 MW PASP were measured as 2.8×10^{-6} and 7.7×10^{-7} cm^2/s, respectively, at pH 3.5. From these values, R_H was calculated as 0.79 and 3.20 nm for 3000 MW and 10 000 MW PASP, respectively.

The influence of polymer concentration on dissolution rate is illustrated in Figures 10 and 11 for dissolution at 1200 and 300 rpm. At pH 3.5 (Figure 10), as PASP concentration increases, the rate of dissolution increases and begins to level off at the highest concentration. Thus, PASP promotes dissolution over the range of concentrations studied here. The rate levels off at 0.1 M PASP because the reaction process begins to limit dissolution, and the polymer chains begin to adsorb in more loops and tails at high concentration. In contrast, at pH 10 (Figure 11), a minimum in the dissolution rate is observed at 0.001 M PASP and above this concentration the rate increases until dissolution is enhanced at 0.1 M PASP. In this pH regime, PASP inhibits dissolution at low concentrations and promotes dissolution at high concentrations. This is similar to the behavior of citrate in calcium phosphate dissolution studies.[8,25]

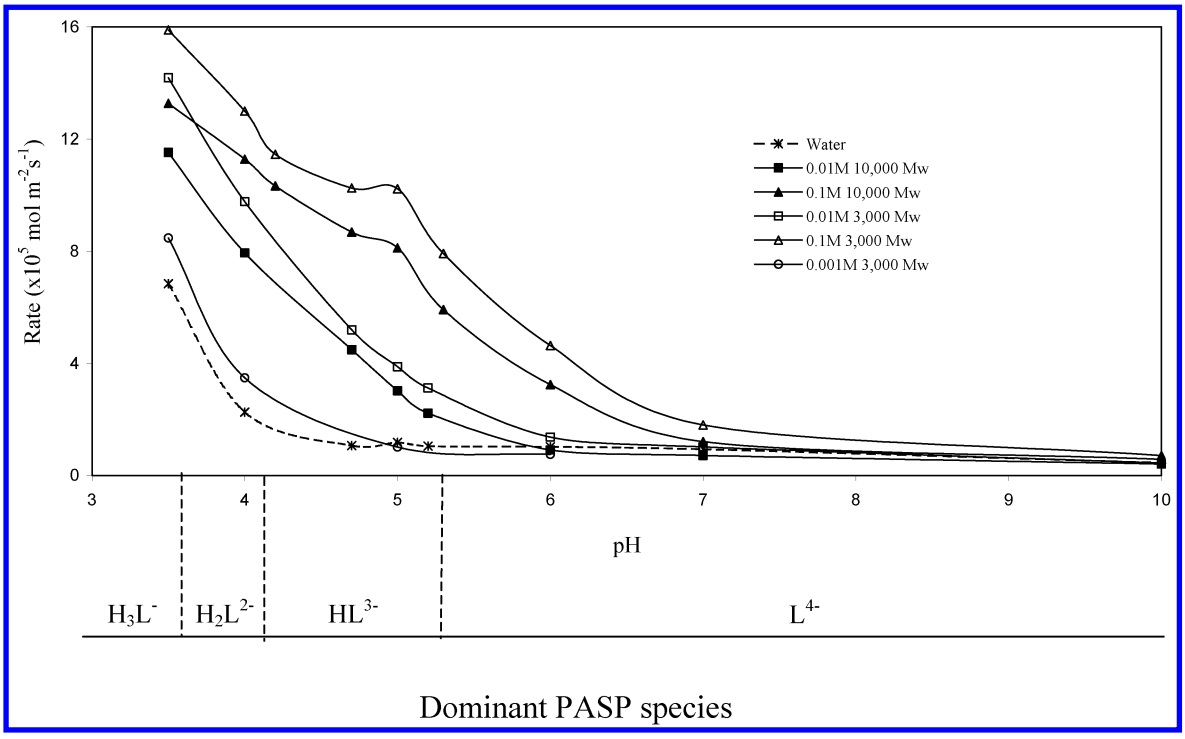

Figure 12. Rate of dissolution over the pH range in the absence and presence of PASP.

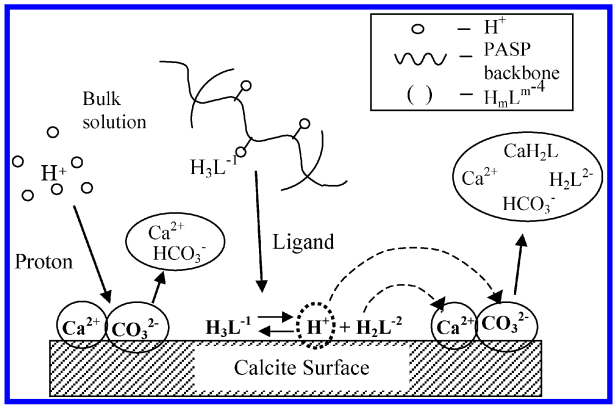

Figure 13. Mechanisms of calcite dissolution in the presence of PASP.

4.2. Proton-Promoted versus Ligand-Promoted Dissolution. The overall effect of pH on dissolution in PASP is demonstrated in Figure 12 for various molecular weights and concentrations of polymer, with smoothed fit lines of the data to show trends. The dominant polymer species at each pH region are represented below the graph to illustrate the effect of chelation chemistry on dissolution. The rate of dissolution is greatest at pH 3.5 and decreases with higher pH, in both the presence and absence of PASP. Interestingly, a local maximum in the rate is observed at pH 5 for both MWs at the highest concentration of polymer. This maximum rate occurs in the pH region where HL^{3-} and L^{4-} are the principal PASP species. Since dissolution at pH 5 in high PASP concentration is limited by both mass transfer and surface reaction kinetics (Figure 7), the mixture of HL^{3-} and L^{4-} yields an optimal combination for H^+ transport, acid attack, and ligand attack.

Calcite dissolution in the presence of polyaspartic acid occurs via different mechanisms at high and low pH conditions. In the proposed overall mechanism (Figure 13), the polymer species H_mL^{m-4} ($m = 3$ in this example, but will depend on pH) travels from the bulk fluid to the interface and subsequently dissociates at the calcite surface, generating H^+ and deprotonated ligand ($H_{m-1}L^{m-5}$). As a result, free calcium, bicarbonate, and calcium−polymer complexes are formed during interfacial reaction. If the Ca−PASP complex is unstable, it collapses in the bulk fluid to release Ca^{2+} and free polymer ligand species. In this case, the principal role of PASP is proton transport and dissociation. However, if the complex is stable, it remains in solution and the primary function of PASP is chelation.

In Figure 14a, plots of calcium concentration versus time from dissolution studies at pH 10 show that while total calcium increases, bulk Ca^{2+} remains at nearly zero, indicating that all calcium in solution is bound to PASP. At this pH, the dominant polymer species in solution is L^{4-}. Since the Ca−PASP binding constant is largest for L^{4-}, this is the most stable metal−ligand complex. Thus, the dissolution of calcium at high pH (>7) is chiefly promoted by complexation.

Comparing this to Figure 14b for dissolution at pH 3.5, we observe that the free calcium concentration is equal to the total calcium concentration, indicating that all calcium is unbound as Ca^{2+}. At this pH, PASP is predominantly in the form of H_3L^- and H_2L^{2-}, which have lower binding constants with calcium than L^{4-}. Upon reaction with calcium at the interface, these less stable complexes (CaH_3L and CaH_2L) break up to release Ca^{2+} and free polymer. In addition to the chelation reaction, PASP also provides additional H^+ for reaction 2, as it undergoes rapid dissociation at the interface. Thus, at low pH, calcium dissolution in the presence of PASP occurs via a combination of chelation and acid attack of the calcite surface.

To quantify the performance of PASP over a range of pHs, we have defined an enhancement factor, η_{enh}, as the ratio of the rate of dissolution in PASP over the rate of dissolution in water. Figure 15 demonstrates that, for various conditions of ω, polymer concentration, and molecular weight, η_{enh} has a maximum at pH ∼ 4.0−4.7.

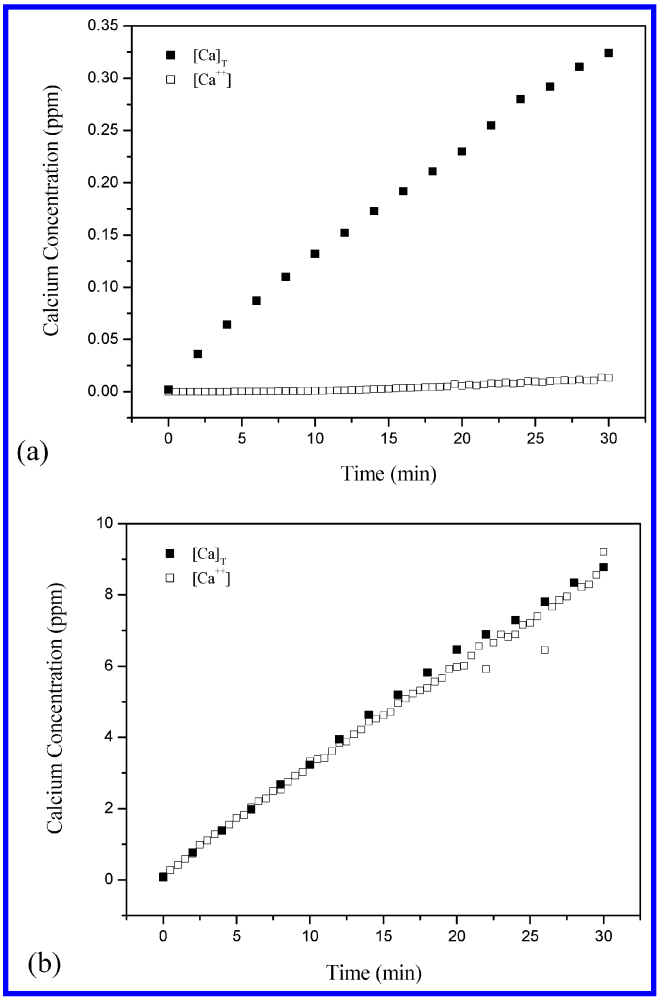

Figure 14. Total (Ca_T) and free (Ca^{2+}) calcium concentration versus time profiles for dissolution at 1200 rpm in 0.01 M PASP 10 000 MW at (a) pH = 10 and (b) pH = 3.5.

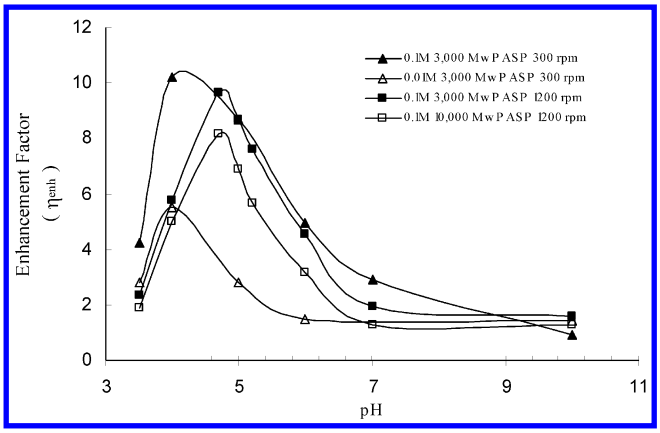

Figure 15. PASP enhancement of calcite dissolution.

(41) Sikes, C. S.; Wierzbicki, A. *Corrosion' 97*, NACE conference paper No. 166, 1997.

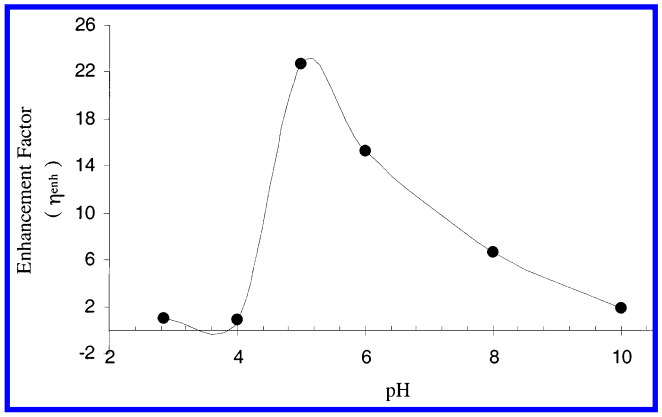

Figure 16. PASP enhancement of brushite (DCPD) dissolution for 600 ppm PASP concentration and 1.2 m/s flow rate.[25]

Similar results are shown in Figure 16 for our earlier research on the dissolution of calcium phosphate from the inner surface of a tube in PASP solution under turbulent flow, with a maximum enhancement at pH ~ 5.[25]

4.3. Surface Morphology. While the rotating disk is a convenient method for investigating the microscopic features of dissolution, it is also useful to examine the macroscopic characteristics of this process. Scanning electron microscopy is a valuable technique for monitoring the evolution of calcite surface morphology during dissolution, which may reveal information on the interactions of various species (e.g. H^+ and PASP) with the calcite surface during dissolution.

Figure 17 represents scanning electron images of calcite disks taken before and after dissolution in both the presence and absence of PASP. In Figure 17a, the calcite surface is polished prior to dissolution. In Figure 17b and c, at pH 3.5, the calcite surface is relatively smooth and uniform for dissolution without polymer, while the surface resulting from dissolution in PASP exhibits a series of pitted holes. In Figure 17d and e, the surfaces are considerably different for dissolution in the absence and presence of polymer at pH 10. The calcite surface dissolved in PASP solution contains many grooves and deep carvings, where the polymer is assumed to attack dislocation sites.

These images clearly demonstrate that calcite dissolution in the presence of PASP occurs via different mechanisms than dissolution without PASP. The polymer attacks and dissolves the surface in a very different manner than water molecules or H^+ ions, consistent with a surface adsorption−complexation reaction mechanism.[2,23] Furthermore, Figure 17e gives substantial evidence that the ligand reaction with calcite dominates at pH 10 for high PASP concentration, as the surface is significantly more pitted and nonuniform than the surface dissolved in water (Figure 17d). It is also apparent that the dissolution process depends strongly on pH, comparing

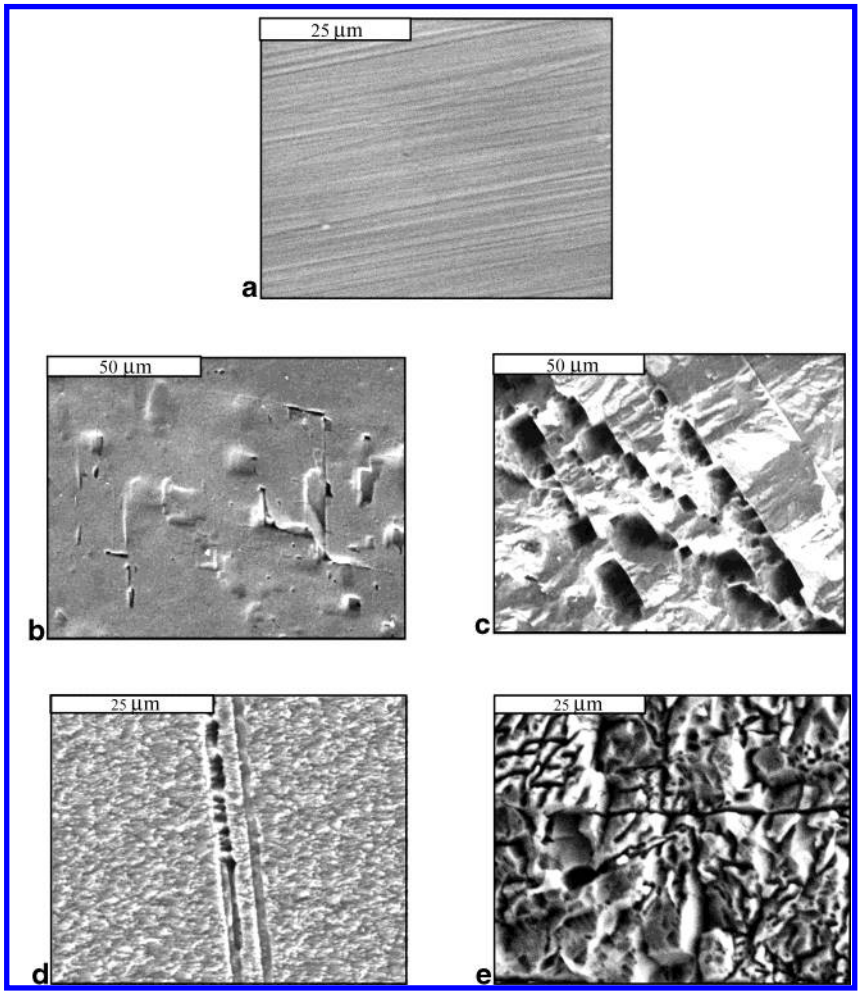

Figure 17. (a) Calcite surface prior to dissolution (2000×). (b) Calcite surface after dissolution in 0 M PASP at pH = 3.5 for 1 h (1000×). (c) Calcite surface after dissolution in 0.1 M PASP (3000 MW) at pH = 3.5 for 1 h (1000×). (d) Calcite surface after dissolution in 0 M PASP at pH = 10 for 3.5 h (2000×). (e) Calcite surface after dissolution in 0.1 M PASP at pH = 10 for 3.5 h (2000×).

images of the calcite surface upon dissolution at pH 3.5 and 10 in the same PASP concentration (Figure 17c and e). This is due to the additional effect of hydrogen ion attack at low pH, similar to that observed by Fredd and Fogler for calcite dissolution in EDTA.[2]

5. Conclusions

Calcite dissolution proceeds most rapidly at low pHs in both the absence and presence of polyaspartic acid. At the lowest pH studied here (3.5), dissolution is governed chiefly by the proton reaction with calcite. At the highest pH (10), dissolution occurs via complexation between calcium and the PASP ligand. Between these extremes, a combination of H^+ and ligand reaction with calcite governs dissolution. In addition, dissolution is mainly surface-reaction-controlled at high pH and mass-transfer-limited at low pH, with increasing interfacial reaction limitations at high PASP concentration. The theoretical model developed in this work further supports the experimental findings at pH 10. The molecular weight of PASP has a more pronounced effect at low pH, where mass transport is the rate-determining step. In this regime, lower molecular weight (3000) PASP increases the dissolution rate mainly due to its higher diffusion coefficient.

Polyaspartic acid is most effective for calcite dissolution in the range of pH $\sim 4-5$, where the enhancement factor, η_{enh}, exhibits a maximum. The parameter η_{enh} is a method to quantify the behavior of the cleaning material in dissolution applications. In the case of PASP, η_{enh} is related to the species distribution and chelation chemistry of PASP as a function of pH. In the pH range for maximum dissolution enhancement, there is an optimal combination of acidic and chelant attack of the calcite surface, as well as enhanced reactant mass transfer. However, over the entire pH range studied, PASP proved an efficient dissolving agent for calcite and is therefore considered a practical and environmentally friendly alternative to current calcium salt cleaning agents.

Acknowledgment. We gratefully acknowledge the following for financial and technical support: the National Science Foundation (NSF),Grant numbers CTS-9905152 and CTS-9912339; the National Institute of Standards and Technology (NIST), Contract number NA1341-02-W-1281; Donlar Corporation for donating sodium polyaspartate; and Durham Marble Company for supplying calcite marble. We also thank Dr. van Zanten of North Carolina State University, Dr. Lee Yu of NIST, and Drs. Robert Pietrangelo and Grace Fan of Donlar for their technical assistance. Finally, we would like to acknowledge undergraduate students Elisa Enders, Lucas Revellon, and Merrick Miles, from North Carolina State University, and Leah Taylor, from the University of Missouri, for their assistance with laboratory experiments. Support for the undergraduate students was provided by the NSF Green Processing REU Program (EEC-9912339) and the Howard Hughes Medical Institute (HHMI).

LA020815G